Journal of Technology and Social Science (JTSS)

Test Mass Verification for Free Fall Interferometers

Sachie Shiomi, Shunsuke Watanabe, Taichi Hikosaka, Tatsunori Yamamoto, Hiroki Chiku, Masaru Sasaki and Kou Yamada

Division of Mechanical Science and Technology, Faculty of Science and Technology, Gunma University, 1-5-1 Tenjin-cho, Kiryu-city, Gunma 376-8515, Japan

Keywords: free fall, gravity gradiometer, centre of mass, weighbridge, interferometer

Abstract. In a free fall interferometer, a test mass or a pair of test masses, which form a part of the interferometer, are put in free fall and the free fall acceleration is measured by the interferometer. In such interferometers, rotations of test masses in free fall could cause a serious disturbance. The rotational disturbance can be minimised by adjusting the location of the centre of mass of each test mass. In previous work, a weighbridge method was applied to locate the centres of mass of prototype test masses for a gravity gradiometer that employs a free fall interferometer. We present a more detailed description of the experiment and measurement results in this paper. Our results show that the uncertainty in the weighbridge method is sufficiently small to verify test mases for the gravity gradiometer that aims to detect differential acceleration to 0.1 μgal or 1×10^{-9} m/s^2.

1. Introduction

Free fall interferometers have been used in various instruments and experiments, such as absolute gravimeters [1, 2], gravity gradiometers [3, 4] and fifth-force searches in fundamental physics [5, 6]. Also, there are prospects to be used to observe gravitational waves in space (e.g. [7]).

In a typical free fall interferometer, one or more test masses, each of which embedded with a retroreflector (such as a corner cube prism or a hollow retroreflector), are put in free fall in high vacuum. Each test mass forms a part of the interferometer. A laser beam is directed onto the retroreflector embedded in each test mass and acceleration of the falling test mass is measured by the interferometer.

When such a test mass, embedded with a hollow retroreflector, is put in free fall with a small unwanted angular velocity ω, it rotates around its centre of mass (Fig. 1). When the optical centre of the retroreflector is offset from the centre of mass of the test mass by d, the change in the length of the optical path in the vertical direction (z-axis) can be expressed as

$$\Delta z(t) = z_1 - z_2 = d(1 - \cos \omega t). \qquad (1)$$

By taking the second derivative of $\Delta z(t)$ with respect to time t, the magnitude of acceleration disturbance due to a small rotation ($\omega t \ll 1$) of the test mass can be given by

$$a_z \approx d \cdot \omega^2. \qquad (2)$$

This rotational acceleration disturbance could be a limiting factor to achieve high sensitivity in free fall interferometers. To minimise the rotational acceleration disturbance, each test mass has to be fabricated so that the offset d is as small as possible. Also, the mechanism that puts test masses in free fall has to be designed to minimise the angular velocity ω. Angular velocity of a test mass in free fall can be measured, for instance, by using an optical lever that employs a four-segment photodiode [4]. This paper focuses on a method of estimating d by measuring the centre of mass of each test mass. This method was briefly introduced in previous work [8]. In this paper, we present a more detailed description of the experiment and measurement results.

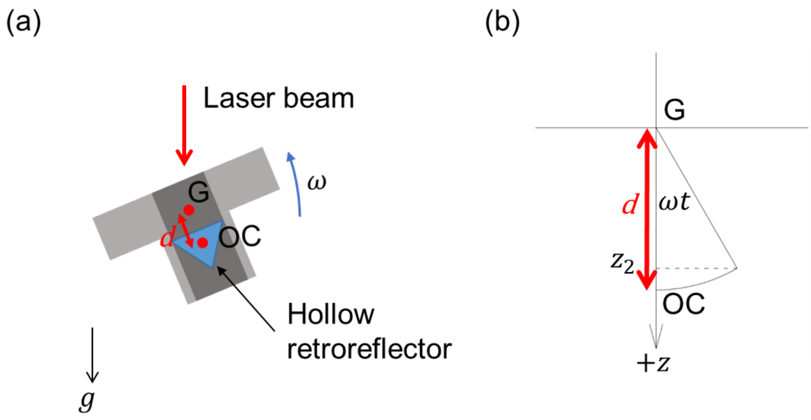

Fig. 1. Rotation of a test mass (a) a schematic cross-section of a test mass (not drawn to scale) falling with a small angular velocity ω (the rotation angle has been exaggerated). A laser beam is incident on the retroreflector embedded in the test mass, in the vertical direction. (b) the change in the length of the optical path in the vertical direction *z*, caused by the rotation of the test mass. Code: OC= optical centre, G= centre of mass of the test mass and *d* = distance between OC and G.

2. Experimental Method

The centre of mass of a 1 kg artefact can be located within a precision of micrometres by using a weighbridge method developed at the Bureau International des Poids et Mesures (BIPM) [9]. This method was applied to locate the centres of mass of prototype test masses for a portable interferometric gravity-gradiometer in the previous work [8]. A more detailed description of the weighbridge method is given in the following sections.

2. 1 Operation Principle

The principle employs a weighbridge, fabricated according to the details given in [9], and an electronic laboratory balance and a solid support (Fig. 2). The left-hand knife of the weighbridge is centred on a brass disc placed on the pan of the balance and the right-hand knife is placed on the solid support. The balance (METTLER TOLEDO, ME4002) has a capacity of 4.2 kg and a resolution of 0.01 g. The pan is kept at a fixed height by servo-control; the height of the pan is independent of load. The brass disc is placed on the pan so that the pan cover will not flex under load.

When a test object is placed on the weighbridge as shown in Fig. 2, there is no net torque about the right-hand knife of the weighbridge in equilibrium. Therefore, the height of the centre of mass of the test object can be given by the following relation [9]:

$$h = \left(\frac{m_0 - m_1}{m_0}\right) L + R_1 \tan\theta_1, \quad (3)$$

where L is the length of the span of the weighbridge, m_0 is the mass of the test object and m_1 is the change in mass indicated by the balance when the test object is placed as shown in Fig. 2; R_1 is the distance between the centre of mass of the test object and the plane defined by the knives of the weighbridge; θ_1 is the tilt angle of the weighbridge with respect to the horizontal direction. The height of the solid support is adjusted to minimise the tilt angle.

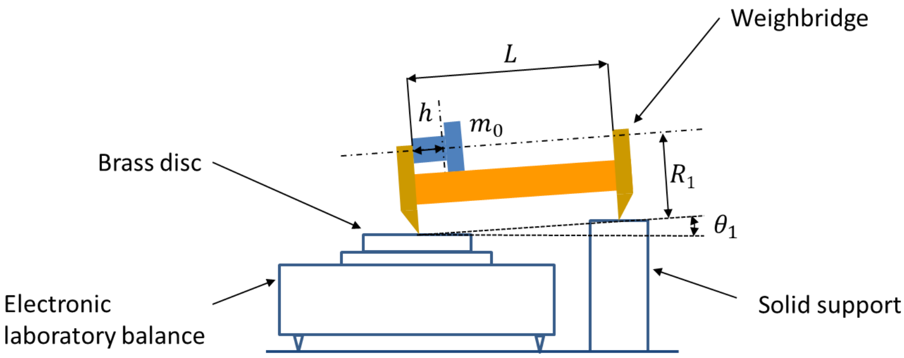

Fig. 2. A schematic view of the first measurement (not drawn to scale). A weighbridge is placed between a brass disc on the pan of an electronic laboratory balance and a solid support. A test object with mass m_0 is set against the left-hand wall of the weighbridge. The height of the solid support is adjusted so that θ_1 is nominally zero (θ_1 has been exaggerated for clarity). The brass disc is placed on the pan to prevent the pan cover from flexing under load. Code: h = height of the centre of mass of the test object, L = span of the weighbridge, R_1 = distance between the centre of mass and the plane determined by the knives of the weighbridge and θ_1 = tilt angle of the span with respect to the horizontal.

When the test object is placed against the right-hand wall of the weighbridge, as shown in Fig. 3, we obtain the following relation in equilibrium [9]:

$$h = \frac{m_2}{m_0} L - R_2 \tan\theta_2, \tag{4}$$

where m_2 is the change in mass indicated by the balance when the test mass is placed as shown in Fig. 3, R_2 is the distance between the centre of mass of the test object and the plane defined by the knives and θ_2 is the tilt angle of the weighbridge with respect to the horizontal direction.

When $\theta_1 = \theta_2$ $(\equiv \theta)$ and $R_1 = R_2$ $(\equiv R)$, the tilt angle can be obtained by eliminating h from Eqs (3) and (4) [9]

$$\tan\theta = \left(\frac{m_1+m_2-m_0}{m_0}\right)\frac{L}{2R}. \tag{5}$$

By eliminating θ from Eqs (3) and (4), the height of the centre of mass of the test object is given by the following relation [9]:

$$h = \left(\frac{m_0-m_1+m_2}{m_0}\right)\frac{L}{2}. \tag{6}$$

We have used this relation for determining h. Relations for $\theta_1 \neq \theta_2$ and $R_1 \neq R_2$ are discussed in Section 2.3.

2.2 Determination of *L*

A brass cylinder having a nominal diameter of 33 mm was used as a standard to determine L. Micrometre measurements show that the height of the standard is $2h_{st}$ = 60.019 ± 0.006 mm at 25.0 °C.

The first and second measurements were carried out by positioning the base of the standard against the left-hand wall and right-hand wall of the weighbridge, respectively, and m_1 and m_2 were obtained.

By substituting the measured values of m_0, m_1, m_2 and $2h_{st}$ into Eq. (6), we have determined L. Such a determination of L was repeated six times before measuring each test object. The mean $\bar{L}$ of L was obtained from the repeated measurements.

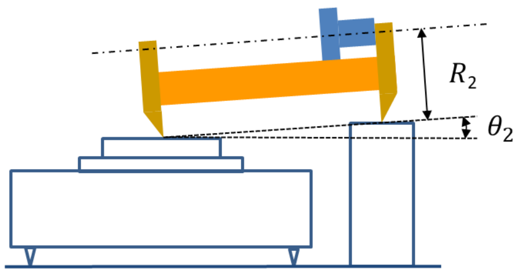

Fig. 3. A schematic view of the second measurement (not drawn to scale). The base of the test object is placed against the right-hand wall of the weighbridge; R_2 is the distance between the centre of mass of the test object and the plane defined by the knives of the weighbridge; θ_2 is the tilt angle of the span with respect to the horizontal (θ_2 has been exaggerated for clarity).

2.3 Estimation of tilt effects

When $R_1 \neq R_2$, Eqs (3) and (4) yield the following relation:

$$h = \left(\frac{m_0 - m_1 + m_2}{m_0}\right)\frac{L}{2} + \frac{(R_1 - R_2)}{2}\tan\theta. \quad (7)$$

This relation indicates that the difference, $\Delta R = R_1 - R_2$, introduces an additional term in the determination of h. The magnitude of this additional term was estimated in the following method that is based on the previous work [9].

Aluminium thin plates were placed under the solid support to set the tilt angle θ to 3.3, 6.7, 10 and 13 mrad. At each angle, m_1 and m_2 of the standard were measured. The measured values were substituted into Eqs (3) and (4), and R_1 and R_2 were estimated, respectively. By least-squares fitting of the estimates obtained under those different tilt angles, we have obtained $R_1 = 43.8 \pm 1.8$ mm and $R_2 = 44.6 \pm 1.7$ mm, thus $\Delta R = -0.8 \pm 2.5$ mm. When θ is less than 0.7 mrad, the magnitude of the additional term is not more than 1 μm and negligible. By substituting calibration data (see Section 2.4 for calibration) into Eq. (5), the average tilt angle θ was estimated to be 0.52 mrad and the additional term is negligible. With the standard placed as shown in Fig. 2 or Fig. 3, height measurements show $R = 41.5$ mm. This value is smaller than the obtained values of R_1 and R_2. This could be due to systematic underestimates of the thickness of the aluminium plates by about 6 %.

When $\theta_1 \neq \theta_2$, Eqs (3) and (4) yield the following relation:

$$h = \left(\frac{m_0 - m_1 + m_2}{m_0}\right)\frac{L}{2} + (\tan\theta_1 - \tan\theta_2)\frac{R}{2}. \quad (8)$$

The magnitude of the last term of Eq. (8) has not been estimated as the difference between $\tan\theta_1$ and $\tan\theta_2$ is not measured by the experiment. Such a difference in the tilt angle could arise, for instance, when shims used for fine levelling of the weighbridge are not set properly or the knives of the weighbridge have some geometrical imperfections; when one end of the left-hand knife is slightly shorter than the other end, the tilt angle would depend on the torque applied to the weighbridge. The standard deviation of a single measurement of θ was about 0.1 mrad in the calibration data. If this amount of difference ($\theta_1 - \theta_2$ = 0.1 mrad) arises, the last term of Eq. (8) gives rise to a spurious effect of 2 μm.

2.4 Calibration and tests

Another brass cylinder with a slot, 3 mm wide and 3 mm deep, cut along a diameter at one end was prepared for calibration. Its nominal diameter is 33 mm and micrometre measurements show that the height is $2h_{sl}$ = 59.976 ± 0.006 mm at 25.0 °C.

Firstly, the span $\bar{L}$ was determined from the measurements of the standard, as described in Section 2.2. Secondly, the first and second measurements of the slotted cylinder were carried out. Using the value of $\bar{L}$, the height of the centre of mass of the slotted cylinder was obtained from Eq. (6). Such a determination of h was repeated six times within a day and the mean of h was obtained. Such a mean of h was determined four times with the slotted end as base and three times with the slotted cylinder reversed.

2.5 Test masses

Two cylindrical test masses (A and B) were prepared for performance tests of a toss-up mechanism developed for the portable interferometric gravity-gradiometer [4]. Each test mass is embedded with a flat mirror with a diameter of 10 mm. The weight of each test mass is about 15 g.

The span $\bar{L}$ was determined by measuring the standard, as described in Section 2.2; then, the first and second measurements of each test mass were repeated six times. The mean of h of each test mass was obtained from the six measurements. Such a determination of the mean was made twice on different days for each test mass.

3. Results and Discussion

Tables 1 and 2 show the measurement results of the slotted cylinder and the test masses, respectively. The measurements were carried out at room temperatures from 22 to 26.5 °C. The magnitude of temperature change was less than 0.5 °C during one determination. The measured values were converted to the ones at 25.0 °C and shown in Tables 1 and 2.

The means $\bar{L}$ determined before measuring the slotted cylinder and the test masses are also given in Tables 1 and 2. The standard deviation of a single measurement of L was not more than 0.03 mm. The uncertainty δL in $\bar{L}$ was estimated by adding in quadrature of the standard deviation of the mean and the uncertainty δL_{p} that propagates as $(L/h)\delta h_{st}$ to L, where δh_{st} is the uncertainty in the height of the standard; δL_{p} was estimated to be 0.015 mm by substituting δh_{st} = 0.003 mm. Uncertainty due to the resolution of the balance is negligible in the determinations of L.

The weighted mean of the seven determinations of $\bar{L}$, five for the slotted cylinder and two for the test masses, was 149.97 ± 0.02 mm, where the uncertainty is the quadratic sum of δL_{p} and the uncertainty obtained by propagating the standard deviations of the means. The uncertainties of the weighted means of $\bar{L}$ shown in Tables 1 and 2 were also obtained in the same manner. The span measured by vernier callipers was 149.90 ± 0.05 mm.

Though the same weighbridge was used throughout the measurements, $\bar{L}$ varied from 149.89 to 150.03 mm (Tables 1 and 2). One of the causes could be some geometrical imperfections of the knives of the weighbridge; they are not perfectly parallel to each other and the points that touch the surfaces of the brass disc and the solid support might have changed during the measurements.

The uncertainty δh in each determination of h was obtained by adding in quadrature of the standard deviation of the mean and the uncertainty δh_{p} that propagates as

$$\delta h_{\mathrm{p}} = \sqrt{\left(\frac{h}{L}\right)^2 (\delta L)^2 + \left(\frac{L}{2m_0}\right)^2 \{(\delta m_1)^2 + (\delta m_2)^2\} + \left(\frac{L}{2} - h\right)^2 \left(\frac{\delta m_0}{m_0}\right)^2}, \tag{9}$$

where δm_0, δm_1 and δm_2 are the uncertainties due to the resolution of the balance. When $\delta m_0 = \delta m_1 = \delta m_2$, we obtain the following relation:

$$\frac{\delta h_p}{h} = \sqrt{\left(\frac{\delta L}{L}\right)^2 + \left(\frac{3}{4}\frac{L^2}{h^2} - \frac{L}{h} + 1\right)\left(\frac{\delta m_0}{m_0}\right)^2}. \tag{10}$$

We used the standard deviation of ± (0.01/$\sqrt{12}$) g (≈ 0.0029 g) for δm_0, δm_1 and δm_2 in the estimates.

We have obtained the weighted means of h_{s} = 30.159 ± 0.004 mm for the measurements with the slotted end as base and h_{r} = 29.832 ± 0.006 mm for the measurements with the slotted cylinder reversed (Table 1). The uncertainty in each of the weighted means is the quadratic sum of δh_{p} and the uncertainty obtained by propagating the standard deviations of the means. The largest contribution to δh was from the uncertainty due to δL, which propagates as $(h/L)\delta L$.

A calculation based on the dimensions of the slotted cylinder shows that the height of the centre of mass of the slotted cylinder is 30.153 ± 0.004 mm from the slotted end and 29.824 ± 0.004 mm from the other end at 25.0 °C. The uncertainties in these calculated values are primarily due to the uncertainty in the micrometre measurements of the height $2h_{\mathrm{sl}}$. The measurement results from the weighbridge method were consistent with the calculated values. However, both of the weighted means were 6 μm or more larger than the calculated values; there could be some systematic effects that have not been considered in the above analyses. The mean tilt angle, obtained from Eq. (5), varied from 0.21 mrad to 0.75 mrad in the determinations given in Table 1. The largest tilt angle was 0.75 ± 0.14 mrad in the fourth determination of h_{s}, where the uncertainty in the tilt angle is the standard deviation of a single measurement. By substituting the largest tilt angle into Eq. (7), the last term in Eq. (7) was estimated to be -0.3 ± 0.7 μm and negligible. If θ_1 is larger than θ_2 by 0.28 mrad, which is twice of the standard deviation of 0.14 mrad, the last term of Eq. (8) will add 6 μm to h. This effect might have caused the overestimates of h. This effect could be reduced, for instance, by using a weighbridge with fewer geometrical imperfections, or by replacing the solid support with another electronic laboratory balance [10]. In the latter method, a weighbridge is placed between two electronic laboratory balances and m_1 and m_2 are measured at the same time using the two balances; in this experimental setup, θ_1 and θ_2 can be regarded as identical.

The largest uncertainty in h_{s} was also seen in the fourth determination (Table 1). The standard deviation of a single measurement of h_{s} was about twice of the ones of the other determinations. Also, the standard deviation of a single measurement of L in the fourth determination was somewhat larger than the other determinations. This could be due to unstable mass reading or poor levelling of the weighbridge. We will investigate the cause further in the future.

We have obtained the weighted mean of 12.08 ± 0.03 mm for the test mass A and 12.04 ± 0.03 mm for the test mass B. The uncertainty in each of the weighted means is the quadratic sum of δh_{p} and the uncertainty obtained by propagating the standard deviations of the means. The dominant contributions to δh were from the uncertainties δm_0, δm_1 and δm_2.

Equations (9) and (10) show that there are two main sources of uncertainty in the weighbridge method: that due to δL, which propagates as $(h/L)\delta L$ to h, and due to the resolution of the balance. The dominant source of uncertainty depends on the mass of the test object. As we have seen, the uncertainties in the means of the slotted cylinder, which weighs about 433 g, were primarily due to δL. However, the uncertainties in the means of the test masses A and B, each of which weighs about 15 g, were dominantly from uncertainties due to δm_0, δm_1 and δm_2.

The uncertainties in the measurements of the test masses A and B could be reduced by shortening the length of the span of the weighbridge. For example, when the length of the span is half of the one used in the above measurements ($L \approx$ 75 mm), δh_{p} would also be half; the contribution of the last term in Eq. (10) reduces and we could measure the heights of the centres of mass of the test masses A and B with an uncertainty of ± 0.01 mm.

The slotted cylinder used for the calibration is much heavier than the test mass A or B. We plan to carry out calibration using another cylinder whose mass is similar to that of the test masses.

The buoyancy force that acts on the test object introduces an additional term of $\rho V \Delta h / m_0$ to Eq. (6), where ρ is the density of the ambient air, V is the volume of the test object and Δh is the distance between the centre of mass and the geometric centre of the test object. The centre of mass and geometric centre of each test mass lie on the axial axis and the magnitude of Δh is less than 1 mm. Therefore, the additional term of air buoyancy correction is less than 0.5 μm and negligible.

Table 1. The span $\bar{L}$ and the height of the centre of mass of the slotted cylinder at 25.0 °C measured with the slotted end as base h_{s} and with the slotted cylinder reversed h_{r}.

	Span $\bar{L}$ [mm]	**h_{s} [mm]**	**h_{r} [mm]**
1st determination	149.911 ± 0.018	n.a.	29.825 ± 0.004
2nd determination	149.893 ± 0.018	30.155 ± 0.004	n.a.
3rd determination	149.982 ± 0.015	30.160 ± 0.004	29.831 ± 0.004
4th determination	150.025 ± 0.020	30.165 ± 0.007	29.841 ± 0.004
5th determination	149.973 ± 0.019	30.159 ± 0.005	n.a.
Weighted mean	149.972 ± 0.015	30.159 ± 0.004	29.832 ± 0.004
Calculated value of *h*	n.a.	30.153 ± 0.004	29.824 ± 0.004

Table 2. The span $\bar{L}$ and the heights of the centres of mass of the test mass A and B at 25.0 °C.

	Span $\bar{L}$ [mm]	**Test mass A *h* [mm]**	**Test mass B *h* [mm]**
1st determination	149.907 ± 0.017	12.11 ± 0.03	12.05 ± 0.03
2nd determination	149.957 ± 0.019	12.06 ± 0.02	12.04 ± 0.03
Weighted mean	149.925 ± 0.019	12.08 ± 0.03	12.04 ± 0.03

The heights of the optical centres (h_{oc}) of the test masses were estimated by measuring the dimensions with a micrometre. The offset of each test mass was estimated by taking the difference between the weighted mean of the height of the centre of mass and h_{oc}, $d = |h - h_{\mathrm{oc}}|$. Angular velocity of a test mass, put in free fall by using the toss-up mechanism of the portable gravity gradiometer, was measured in the previous work [4]. By substituting the largest angular velocity, ω = 1.0 ± 0.4 mrad/sec, reported in the previous work [4] into Eq. (2), rotational acceleration disturbance was estimated for each test mass; the results are shown in Table 3. The largest rotational acceleration disturbance was estimated to be not more than 0.03 μgal (or 3×10^{-10} m/s^2), which is sufficiently smaller than the current target of the portable gravity gradiometer, 0.1 μgal.

The requirement for d could be more stringent for gravity gradient mapping, as the angular velocity of a test mass seems to be larger on a platform for mapping [11]. We intend to adjust the lengths of the test masses to minimise the offsets. Also, we plan to prepare test masses heavier than the test masses A and B for future measurements so that d can be adjusted more precisely.

When d is minimised, the level of rotational acceleration disturbance would be not more than 3×10^{-11} m/s^2. This indicates that the universality of free fall of two test masses, made of different chemical compositions, could be tested to a level of several parts in 10^{12} by minimising d of the test masses. This corresponds to about two orders of magnitude improvements compared with previous ground-based free fall experiments [5, 6]. To achieve a comparable sensitivity of the best ground tests of the universality of free fall, using torsion balances [12, 13], the magnitude of ω has to be reduced by a factor of 3. To achieve the upper limits placed by a recent space test [14], ω has to be reduced by a factor of ten.

In the portable gravity gradiometer, the location of the centre of mass of the optical table seems to affect the magnitude of the acceleration disturbance [15]. The weighbridge method could also be used to locate the centre of mass of the optical table.

Table 3. The optical centres h_{oc} and offsets d $(= |h - h_{oc}|)$ at 25.0 °C, and rotational acceleration disturbances estimated by using the angular velocity of $\omega =$ 1.0 ± 0.4 mrad/sec reported in [4].

			Test mass A	Test mass B
Optical centre	h_{oc}	[mm]	11.911 ± 0.006	11.911 ± 0.006
Offset	d	[mm]	0.17 ± 0.03	0.13 ± 0.03
Rotational acceleration disturbance	a_z	[μgal]	0.017 ± 0.014	0.013 ± 0.011

4. Conclusion

The centres of mass of the test masses prepared for performance tests of the interferometric gravity gradiometer were measured by using the weighbridge method developed for kilogram standards at the BIPM. The offset of the optical centre from the centre of mass was estimated for each test mass and its rotational acceleration disturbance was estimated for the gravity gradiometer. The largest rotational acceleration disturbance was estimated to be not more than 0.03 μgal. This level of disturbance is sufficiently small for the gravity gradiometer, and also for absolute gravimeters, whose accuracy is a few μgal.

Acknowledgements

This work was supported by KAKENHI Grant Numbers 24684034 and 18K04653, and General Collaborative Research of the Disaster Prevention Research Institute, Kyoto University. One of us (S. S.) would like to thank K. Yamamoto, M. Iguchi, D. Miki and Y. Fujii for valuable discussions and H. Tamura for the technical support.

References

[1] T. M. Niebauer, G. S. Sasagawa, J. E. Faller, R. Hilt and F. Klopping, “A new generation of absolute gravimeters”, ***Metrologia***, Vol. 32, pp. 159-180, 1995.

[2] Micro-g Solutions, Inc: http://microglacoste.com/product/fg5-x-fgl-absolute-gravimeter/

[3] S. Shiomi, K. Kuroda, S. Telada, T. Tsubokawa and J. Nishimura, “Development of a Laser-interferometric Gravity-gradiometer”, ***Journal of the Geodetic Society of Japan***, Vol. 58, No. 4, pp. 131-139, 2012.

[4] K. Seto, S. Shiomi, Y. Kimura, K. Xue, T. Hikosaka, S. Watanabe and K. Yamada, “Performance evaluation of a toss-up mechanism for free-fall interferometers”, ***Proceedings of International Conference on Mechanical, Electrical and Medical Intelligent System 2017***, Invited paper, I10-01, 2017.

[5] K. Kuroda and N. Mio, “Test of a composition-dependent force by a free-fall interferometer”, ***Phys. Rev. Lett.***, Vol. 62, No. 17, pp. 1941-1944, 1989.

[6] K. Kuroda and N. Mio, “Limits on a possible composition-dependent force by a Galilean experiment”, ***Phys. Rev. D***, Vol. 42, pp. 3903-3907, 1990.

[7] LISA mission: https://www.lisamission.org/

[8] S. Shiomi, “Measurement of the centres of mass of test masses for free-fall interferometry”, ***Proceedings of International Conference on Technology and Social Science 2018***, Invited paper, I02-01, 2018.

[9] R. S. Davis, “Device to locate the centre of mass of a test object to within a precision of micrometres” ***Meas. Sci. Technol.***, Vol. 6, pp. 227-229, 1995.

[10] S. Shiomi, “Performance tests of a weighbridge method to locate the centre of mass of a test mass for free-fall interferometry”, ***Proceedings of International Conference on Mechanical, Electrical and Medical Intelligent System 2018***, IPS5-01, 2018.

[11] Y. Matsuda, S. Shiomi, T. Yamamoto, T. Hikosaka, S. Watanabe, H. Chiku, M. Sasaki, K. Xue and K. Yamada, “Development of a platform for gravity gradient mapping”, ***Proceedings of International Conference on Technology and Social Science 2019***, Invited paper, I02-01, 2019.

[12] S. Schlamminger, K.-Y. Choi, T. A. Wagner, J. H. Gundlach and E. G. Adelberger, “Test of the Equivalence Principle Using a Rotational Torsion Balance”, ***Phys. Rev. Lett.***, Vol. 100, 041101, 2008.

[13] T. A. Wagner, S. Schlamminger, J. H. Gundlach and E. G. Adelberger, “Torsion-balance tests of the weak equivalence principle”, ***Classical and Quantum Gravity***, Vol. 29, 184002, 2012.

[14] P. Touboul *et al.*, “MICROSCOPE Mission: First Results of a Space Test of the Equivalence Principle”, ***Phys. Rev. Lett.***, Vol. 119, 231101, 2017.

[15] S. Watanabe, S. Shiomi, T. Hikosaka, K. Xue, T. Yamamoto, Y. Matsuda and K. Yamada, “Reducing acceleration disturbance in a free-fall interferometer by adjusting the location of the center of mass of its optical table”, ***Proceedings of International Conference on Mechanical, Electrical and Medical Intelligent System 2018***, IPS5-02, 2018.